ACS APPLIED MATERIALS & INTERFACES

www.acsami.org

Research Article

Adsorptive Separation of CO_2 by a Hydrophobic Carborane-Based Metal–Organic Framework under Humid Conditions

Lei Gan,[§] Eduardo Andres-Garcia,[§] Guillermo Mínguez Espallargas,* and José Giner Planas*

Cite This: *ACS Appl. Mater. Interfaces* 2023, 15, 5309−5316

Read Online

ACCESS | Metrics & More | Article Recommendations | Supporting Information

ABSTRACT: We report that the carborane-based metal−organic framework (MOF) ***m*CB-MOF-1** can achieve high adsorptive selectivity for CO_2:N_2 mixtures. This hydrophobic MOF presenting open metal sites shows high CO_2 adsorption capacity and remarkable selectivity values that are maintained even under extremely humid conditions. The comparison of ***m*CB-MOF-1'** with MOF-74(Ni) demonstrates the superior performance of the former under challenging moisture operation conditions.

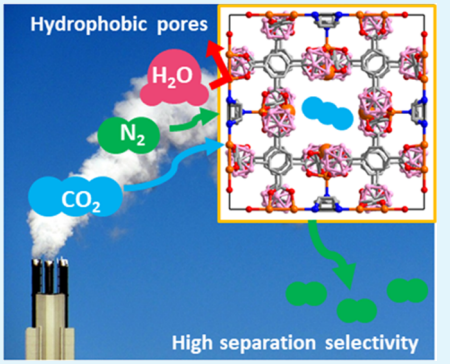

KEYWORDS: *metal−organic frameworks, carboranes, hydrophobic, selective gas separation, breakthrough, humid conditions, CO_2 adsorption*

INTRODUCTION

The global greenhouse effect, which is mostly caused by the emission of CO_2 into the atmosphere, has attracted more and more attention.[1] Apart from natural processes, the consumption of carbon-based fossil fuels from power plants is mainly responsible for generating this anthropogenic CO_2 emission.[2,3] Therefore, carbon capture and storage (CCS) from the postcombustion flue gas is a wise method to reduce CO_2 environmental impact. So far, a number of technologies and materials have been developed for CO_2 capture and separation, such as aqueous ammonia and amine-functionalized solid adsorption,[4−6] membrane separation,[7,8] cryogenics distillation,[9−11] among others. Compared with traditional techniques, adsorption-based methods using porous materials to capture or separate CO_2 with less energy consumption and cost shows great advantages among these technologies. Activated carbon, zeolites, and carbon molecular sieves have been extensively studied as adsorbents for CO_2 separation.[12−14] These materials present several drawbacks such as difficult regeneration procedures and, quite importantly, poor tunability with the procedure conditions. Thus, developing economical and highly regenerative materials to efficiently capture and separate CO_2 from flue gas is highly desirable.

Metal−organic frameworks (MOFs) exhibit outstanding separation performances toward diverse binary gas mixtures due to their large surface areas, tunable pore size and pore surface, and existing open metal sites.[15−18] Many MOFs have been reported to efficiently separate CO_2:N_2 mixtures under dry conditions; however, their performance cannot be often maintained under humid conditions.[19,20] The reason for such a decrease in performance can be twofold. On one hand, there are MOFs that are unstable upon exposure to water and thus cannot be used in gas separation under humid conditions. This is the case, for example, of two of the most well-known adsorbents, HKUST-1 ($[Cu_3(BTC)_2]_n$, BTC^{3-} = benzene-1,3,5-tricarboxylate)[21] and MOF-5 ($Zn_4O(BDC)_3$, BDC^{2-} = 1,4-benzodicarboxylate).[22] The reason for such reduced separation performance under humid conditions is the collapse of the framework by slow hydrolysis when exposed to moisture conditions, even to limited amounts of water. On the other hand, there are other MOFs built by a robust metal cluster that are water-stable, but a common decrease of CO_2 capacity and selectivity is also observed under humid conditions.[23−26] For instance, CO_2 adsorption capacity on UiO-66-NH_2 decreased 88% at 70% RH compared to that at dry conditions.[10] Considering that flue gas contains 5−7% water, these MOFs can only be used for CO_2 separation after a dehydration pretreatment of the gas stream, certainly increasing the economic costs and energy demand of the separation process. Consequently, new approaches are being investigated to

Received: November 15, 2022
Accepted: January 11, 2023
Published: January 24, 2023

increase the robustness of these MOFs absorbents and maintain their water stability, such as alkylamine grafting[27] or PEI composite impregnation.[28] In addition, functionalizing the original linker using hydrophobic functional groups such as fluorine or alkyl groups offers an opportunity to improve the hydrolytic stabilities and repel competitive water molecules from entering into MOFs. However, this methodology requires a more complicated organic synthesis reaction for obtaining the functionalized organic linker.[29−31] Given that water vapor is inevitable among most industrial flue gas mixtures, the screening of facile synthesizable water-stable MOFs for efficient CO_2 separation under humid conditions is both essential and challenging.

Icosahedral carboranes 1,*n*-$C_2B_{10}H_{12}$ (*n* = 2 (*ortho* or *o*), 7 (*meta* or *m*), or 12 (*para* or *p*)) are a class of commercially available and exceptionally stable 3D-aromatic boron-rich clusters that possess material-favorable properties such as thermal and chemical stability and high hydrophobicity.[32−37] Carborane-based linkers in MOFs were first reported in 2007 at Northwestern University.[38] The same group developed a family of thermally robust *p*-carborane-based MOFs over the following years,[39−45] some of those showing high gas sorption capacities and good sieving behavior for gas mixtures. However, the use of the highly expensive and more symmetric *p*-carborane as a scaffold for ligand synthesis prevents any further research on potential real-world applications.[46] Since 2016, some of us have pioneered the use of the cheaper *o*-[47,48] and *m*-carborane[49−55] derivatives with the primary objective of increasing the water stability of the prepared MOFs. We have demonstrated that introducing carborane moieties into MOFs can greatly enhance the framework's water stability. The high hydrophobicity of some of these MOFs has provided them with high hydrolytic stabilities that allow their use in applications where water is always present. This is the case of the *m*-carborane-based $[Cu_2(m\text{CB-L})_2(\text{DABCO})_{0.5}(H_2O)]$ (***m*CB-MOF-1**; *m*CB-L = 1,7-di(4-carboxyphenyl)-1,7-dicarba-closo-dodecaborane; DABCO = 1,4-diazabicyclo[2.2.2]octane; Figure 1), which remains intact in water solutions under very harsh conditions.[52]

In this work, we have investigated our hydrophobic ultra-microporous *meta*-carborane-based MOF (***m*CB-MOF-1**) for gas adsorption and CO_2 separation applications. We show that ***m*CB-MOF-1** exhibits unaffected performance for CO_2:N_2 separation under various humid conditions, validating the results by breakthrough dynamic separation experiments. Regeneration is also successfully achieved in mild conditions despite the presence of water, making this MOF a potential candidate for efficient CO_2 separation from flue gas in industrial applications. The performance of our material is also compared with the well-known water-stable MOF-74(Ni) and shows that ***m*CB-MOF-1** is a superior adsorbent for the separation of CO_2:N_2 mixtures under humid conditions.

RESULTS AND DISCUSSION

***m*CB-MOF-1** shows a rigid twofold interpenetrated porous structure based on $Cu_2(OOC)_4$ paddle wheel units connected via four carborane-based dicarboxylate ligands, resulting in a square network. DABCO ligands connect to only one Cu atom of each paddle wheel, thus providing available Cu open sites (Figure 1).[52] Such a structure differs from other related DABCO pillar-layered MOFs, such as $[M_2(1,4\text{-bdc})_2(\text{DABCO})]$ (M = Ni, Zn; 1,4-H_2bdc=1,4-benzenedicarboxylic acid),[56,57] that do not contain open metal sites. The

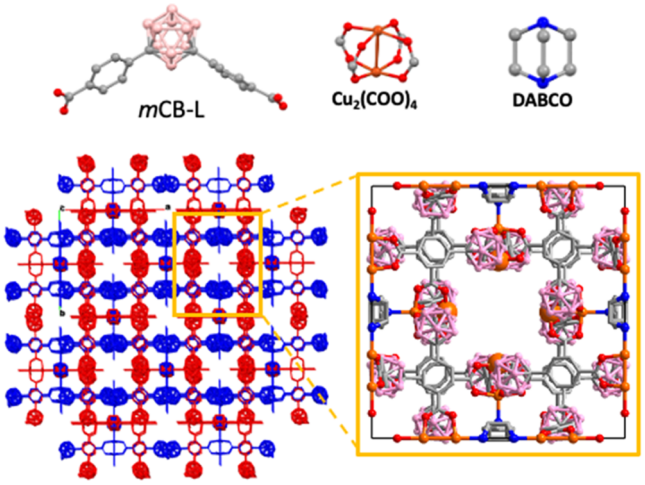

Figure 1. Representation of building units (top) and 3D structure (bottom) of ***m*CB-MOF-1**. Interpenetrated networks are colored blue and red for clarity. The yellow square shows the detail for the pore details along the *c*-axis showing the environment of four Cu_2 paddle wheel units (enlarged orange spheres) surrounded by carborane moieties. Color codes: Cu, orange; B, pink; C, gray; N, blue; O, red. H atoms are omitted for clarity.

highly hydrophobic carborane moieties decorate the 1-D square MOF channels in ***m*CB-MOF-1**, thus providing protection to the Cu_2 paddle wheel units against hydrolysis or ligand displacement. Guest-free ***m*CB-MOF-1**, denoted ***m*CB-MOF-1′**, can be generated by heating at 120 °C in a vacuum and thus provide unsaturated Cu sites. As previously established, ***m*CB-MOF-1′** shows negligible water sorption and has a Brunauer−Emmett−Teller (BET) surface area and pore volume of 756 $m^2\ g^{-1}$ and 0.31 cm^3/g, respectively, and it is also porous to CO_2 (1.34 mmol g^{-1} at 313 K and 2 bar). It is stable in air for at least two years and submerged in 90 °C water for over two months.

Although high hydrolytic stability is a prerequisite for applications where water is present, effective gas separation and good selectivities are not granted. Thus, we first evaluated the ability of ***m*CB-MOF-1′** to separate CO_2 from N_2 by single-gas isotherms measurements. Thus, CO_2 and N_2 sorption data at different temperatures and low pressure were collected (Figure 2a,b). At 1 bar, the CO_2 uptakes on ***m*CB-MOF-1′** were 2.15, 1.35, 0.97, and 0.80 mmol/g at 273, 298, 303, and 313 K, respectively, these values being compatible with those of other ultra-microporous MOFs. When compared with N_2 adsorption, the CO_2 uptake was much higher at 273 K, as shown in Figure 2c, with the adsorption amount of 2.15 mmol/g for CO_2 and 0.21 mmol/g for N_2 at 1 bar at the same temperature. These results demonstrate that CO_2 molecules have higher affinity with ***m*CB-MOF-1′** compared to N_2, highlighting its advantage for highly effective separation of CO_2 from N_2.

To evaluate the evidenced adsorption affinity of the adsorbate−adsorbent, the isosteric heats of adsorption (Q_{st}) for both gases were derived from the static isotherms at different temperatures on the basis of the virial method (see details in Experimental Section and SI). As shown in Figure 2d, the Q_{st} value of CO_2 was in the range of 24.7−25.3 kJ/mol, while the value of Q_{st} for N2 was in the range of 8.2−8.5 kJ/mol, indicating a much stronger interaction between CO_2 and ***m*CB-MOF-1'**, compared to N_2. The zero-coverage Q_{st} for CO_2 was 24.7 kJ/mol, which is lower than that for the related

https://doi.org/10.1021/acsami.2c20373
ACS Appl. Mater. Interfaces 2023, 15, 5309−5316

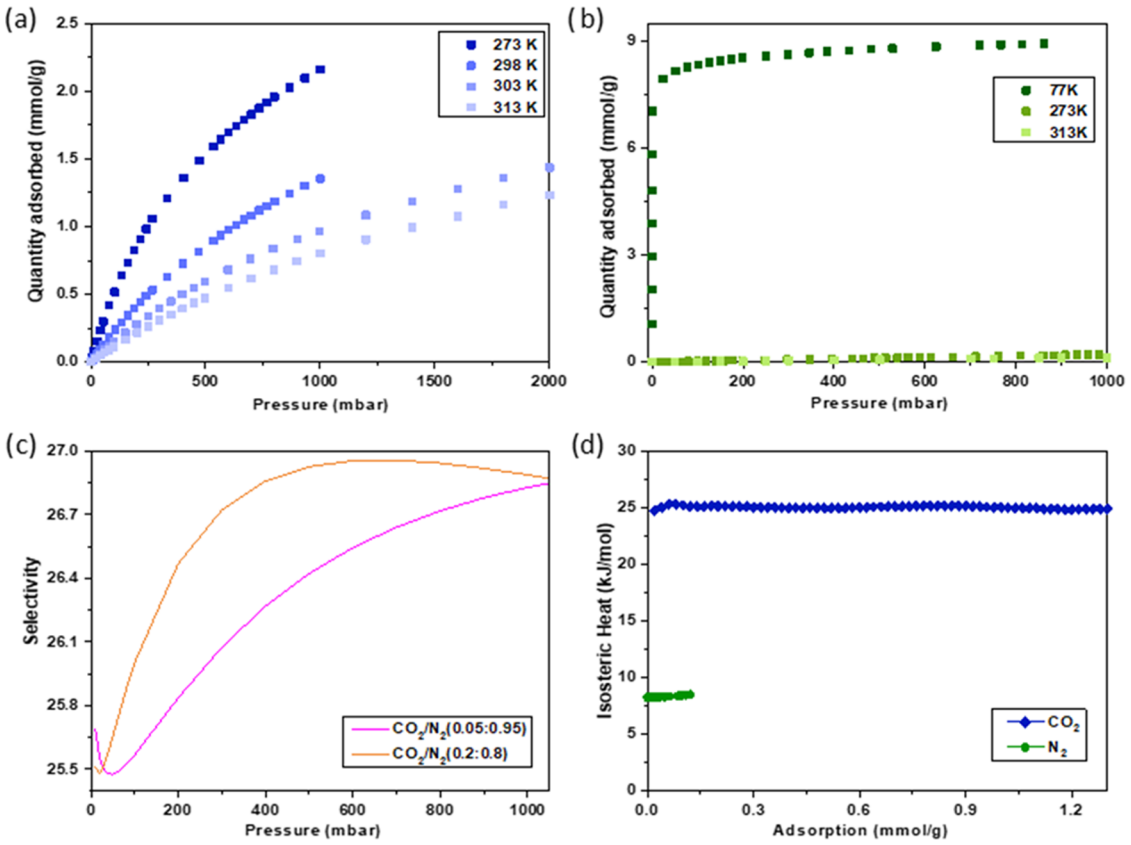

Figure 2. CO_2 (a) and N_2 (b) adsorption isotherms for ***m*CB-MOF-1′** at various temperatures. (c) IAST-predicted selectivities for CO_2:N_2 (0.05:0.95 and 0.2:0.8, v/v) on ***m*CB-MOF-1′** at 273 K. (d) Isosteric heats of adsorption for CO_2 and N_2 on ***m*CB-MOF-1′**.

Cu_2-paddle-wheel-based MOF HKUST-1, showing also open Cu sites. The relatively low Q_{st} for CO_2 suggests that the regeneration process of ***m*CB-MOF-1'** would be easily achieved and with a low energy penalty.

Based on the adsorption performance difference for CO_2 and N_2, an ideal adsorbed solution theory (IAST) was adopted to predict the adsorption selectivity of theoretical CO_2:N_2 binary mixtures. The adsorption isotherms of CO_2 and N_2 were first fitted by dual-site Langmuir−Freundlich isotherm models (see details in Experimental Section and SI). The obtained fitting parameters are summarized in Table S1. It was noticed that both regression coefficients R^2 were higher than 0.9999, indicating the excellent fitting of the data. Figure 2c shows the IAST selectivities at 273 K for CO_2:N_2 (with two different compositions: 0.05:0.95 and 0.2:0.8, v/v) in the pressure range 0−1 bar. Slightly lower CO_2:N_2 adsorption selectivities at lower pressures were observed. At 1 bar, the CO_2:N_2 adsorption selectivity at 273 K was in the range 25.5−27.0, with maximum values of 26.8 and 26.9 for the CO_2:N_2 ratios of 0.05:0.95 and 0.2:0.8, respectively. Nevertheless, there was no significant difference in the adsorption selectivities for the two ratios of gas mixtures. Overall, these results show that ***m*CB-MOF-1'** may exhibit good separation performance of CO_2 from N_2.

Breakthrough measurements are commonly used to evaluate the potential of porous materials in gas separation processes in different conditions. CO_2:N_2 gas mixtures were passed through a fixed-bed column that was filled with 200 mg (average) of ***m*CB-MOF-1'**. Breakthrough operation conditions ranged from 283 to 298 K, at 1 bar, in dry and humid conditions. The inlet mixture was set to a 15 mL min^{-1} flow of a dilution of CO_2 in N_2 (5, and 20%), and completed with an extra 1 mL min^{-1} of helium, used as a nonadsorbing trace. The use of a tracer is mandatory to assure the good performance of the measurement, setting time zero after it breaks through the column. In a typical experiment, the MOF sample was regenerated before the measurement at atmospheric temperature and pressure conditions of 15 mL min^{-1} Ar flow for 20 min. **Dry*m*CB-MOF-1** was activated at 393 K in a vacuum for 2 h. As moisture is a common pollutant in industrial gas flows, ***m*CB-MOF-1** has been investigated under various conditions as shown in Figure 3.

We first conducted CO_2:N_2 breakthrough experiments at two different CO_2 dilutions (5 and 20%) and two temperatures (283 and 298 K) using **dry*m*CB-MOF-1′** (Figures 3a, 4a,b, S1, and Table S2) and a mass spectrometer to measure the outlet gas concentration (Figure 4c). The breakthrough curves indicate that ***m*CB-MOF-1′** could effectively separate the two distinct CO_2:N_2 mixtures under ambient conditions. The N_2 breakthrough occurred first and subsequently reached a plateau early. In comparison, the CO_2 breakthrough time is significantly longer, confirming the effective separation performance of ***m*CB-MOF-1′**. The typical roll-up effect especially appears at a high concentration (20% CO_2, Figures 4b and S1b). CO_2 selectivity is clearly observed also at the lower temperature of 283 K (Figure S1), as it also takes longer for this gas to breakthrough the column. As thermodynamically expected, a significant increase in the amount of adsorbed CO_2 was observed at this temperature (Figure 4c and Table S2), a consequence of adsorption being an exothermic process. This remarkable selectivity (>1000; due to the negligible value of nitrogen adsorption), likely caused by the presence of open

https://doi.org/10.1021/acsami.2c20373
ACS Appl. Mater. Interfaces 2023, 15, 5309−5316

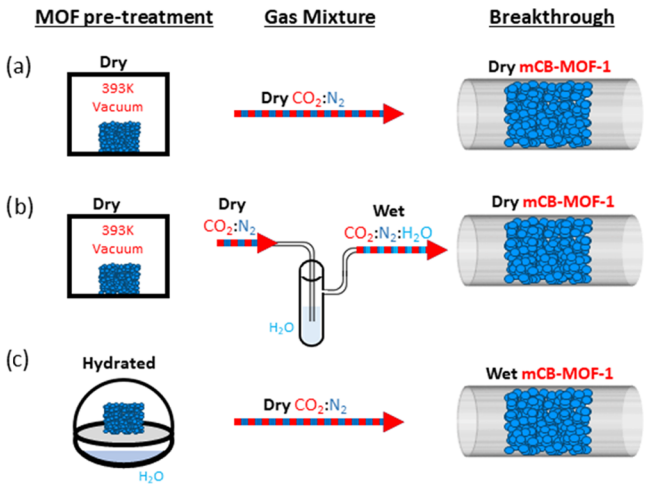

Figure 3. Schematic representation of MOF pretreatment (activated by heating under vacuum (a–c) and prehydrated under a water-saturated atmosphere for 24h (c)) and gas mixture composition (dry CO_2:N_2 (a and c), CO_2:N_2:H_2O (b)) used in the breakthrough experiments.

metal sites (OMS), makes ***m*CB-MOF-1'** a promising material in CO_2:N_2 mixture separation. In addition, increasing the temperature, which favors the diffusion of the gases, causes a reduction in the CO_2 capacity (see Figure 4c), but the selectivity remains very high. Thus, it is clear that the MOF acts as a molecular sieve, avoiding N_2 adsorption and promoting CO_2 capture in gas streams.

The considerable CO_2:N_2 separation performance combined with the hydrophobicity of ***m*CB-MOF-1'** prompted us to investigate the gas separation under high-humidity conditions. For that purpose, two different prehumidification steps were taken. (i) **Wet-gas mixtures**: CO_2:N_2 mixtures were passed through a bubbler containing room-temperature DI water (Figure 3b), assuring that ***m*CB-MOF-1′** was in permanent contact with a hydrated gas stream during the measurement. (ii) **Hydrated*m*CB-MOF-1′**: the sample was prehydrated under a water-saturated atmosphere (100% humidity) for 24 h and before the breakthrough experiments (Figure 3c). Whereas conditions in (i) are close to industrial gas flows, those in (ii) will pose a real challenge for this water-stable adsorbate selectivity, as, in the case of ***m*CB-MOF-1′**, the active sites are open Cu sites with high affinity for water molecules.[58] Thus, we performed the dynamic breakthrough measurements under the same conditions as those for **dry*m*CB-MOF-1′** (5 and 20% CO_2 dilutions; 283 and 298 K). The results (Figures 5, 6, S2, and S3 and Table S2) show that there are no significant differences in the amount of absorbed CO_2 between the **dry**, **wet-gas**, or **hydrated*m*CB-MOF-1′**, evidencing the remarkable water resistance of the adsorbent and CO_2:N_2 separation performance even under high humidity (100% RH). Water is excluded from the pores due to the high hydrophobicity of the MOF channels. This leaves the open Cu sites available for the selective sorption of CO_2 over N_2.

Breakthrough curves and times of the **hydrated*m*CB-MOF-1′** (Figure 5) are nearly identical to those for dry ***m*CB-MOF-1′** (Figure 4). These experimental results further demonstrate that water does not effectively enter the pores of our MOF nor affects the CO_2:N_2 separation selectivities during the breakthrough experiments. Effective separation and good selectivities were also obtained when using wet-gas mixtures (Figure

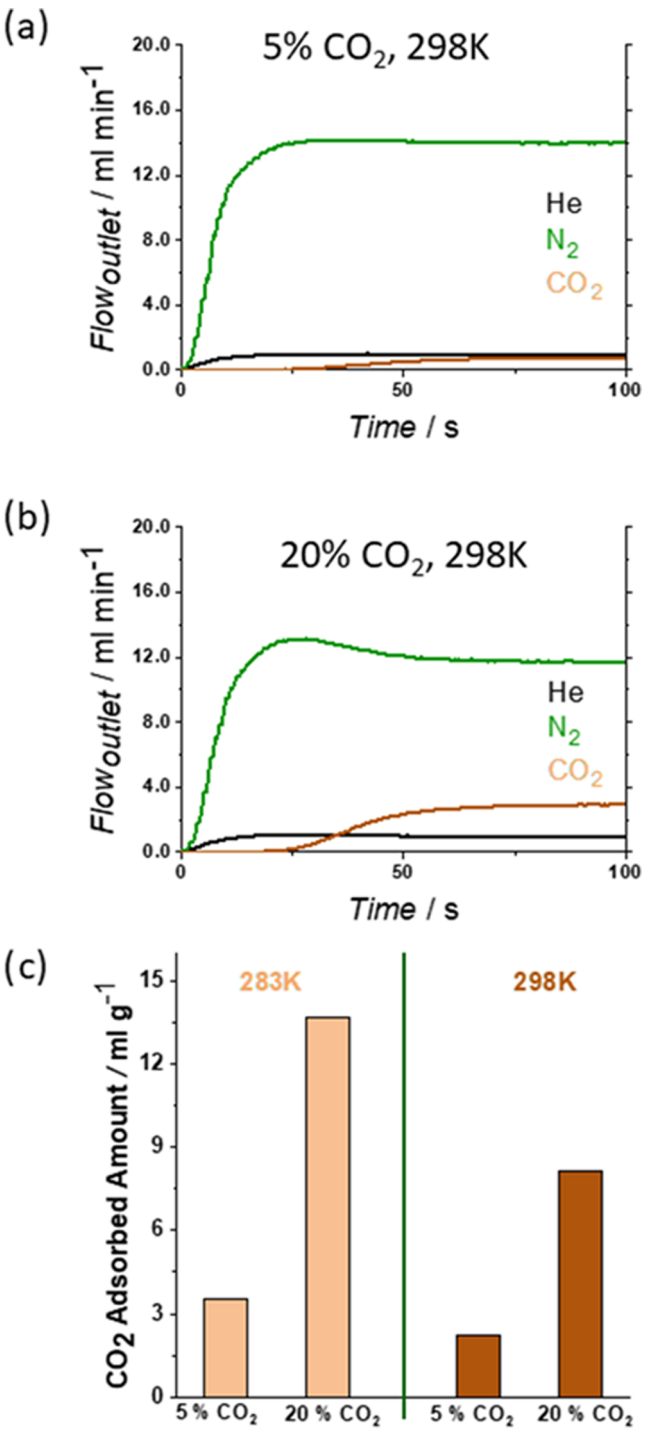

Figure 4. Breakthrough exit flow rates for **dry*m*CB-MOF-1′** at 298 K (5% CO_2 (a); 20% CO_2 (b)) and 1 bar. Time zero is set with the first detection of helium (tracer). (c) Amount of gas adsorbed on **dry*m*CB-MOF-1′** calculated from breakthrough profiles (a) and (b).

S3). During the separation time, the outlet concentration of N_2 is higher than 99%, indicating the outstanding separation for CO_2:N_2 even under humid conditions. Meanwhile, the CO_2 longer break time confirms that the interaction between CO_2 and ***m*CB-MOF-1'** is stronger than that of N_2. Additionally, the captured amount of CO_2 was of the same order (Figure 6) when using wet-gas mixtures or **hydrated*m*CB-MOF-1′** or **dry*m*CB-MOF-1′**. Regeneration tests show that the separation performance was maintained after the adsorption–desorption

https://doi.org/10.1021/acsami.2c20373
ACS Appl. Mater. Interfaces 2023, 15, 5309–5316

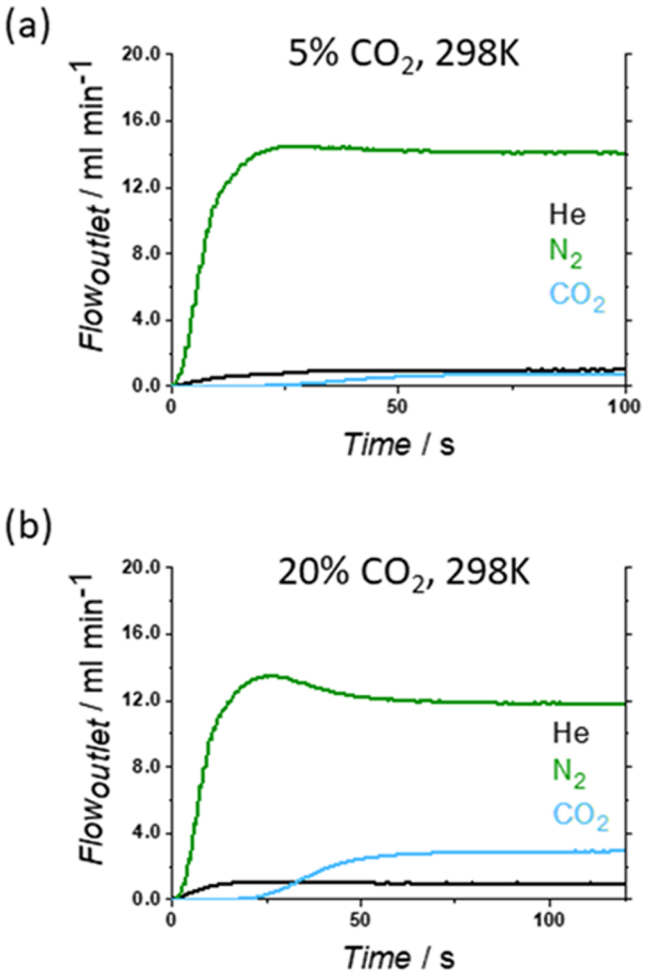

Figure 5. Breakthrough exit flow rates at 298 K and 1 bar on **hydrated*m*CB-MOF-1′**. Inlet composition corresponds to a 5% (a) or 20% (b) dilution of CO_2 in nitrogen.

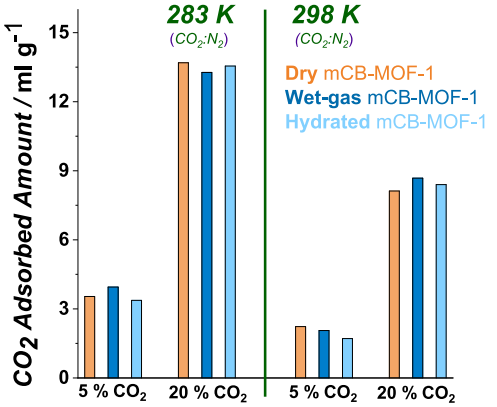

Figure 6. Amount of gas adsorbed on ***m*CB-MOF-1'** (dry and humid conditions) calculated from breakthrough profiles at 1 bar (absolute pressure) for CO_2:N_2, at different concentrations (CO_2: 5−20%), and different temperatures (283−298 K). Time zero is set with the first detection of helium (tracer).

cycles (Figure S4) and the crystalline phase of ***m*CB-MOF-1′** was preserved after the separation process (Figure S5). These experimental results demonstrate that ***m*CB-MOF-1** is a promising porous absorbent for CO_2 separation over N_2 for industrial processes.

Other MOFs with unsaturated metal centers in their structures, such as the MOF-74 family, are recognized as good candidates for the efficient postcombustion CO_2 capture from water-containing flue gas generated from coal-fired power plants.[59,60] From this family of MOFs, MOF-74(Ni) is one of the most water-stable ones.[61,62] We have therefore selected MOF-74(Ni) as a reference material for a comparison study with our ***m*CB-MOF-1′** and performed dynamic breakthrough experiments on dry and hydrated MOF-74(Ni) samples (Figure 3a,c, respectively). Although the MOF remains stable at these conditions, the results represented in Figure 7 clearly

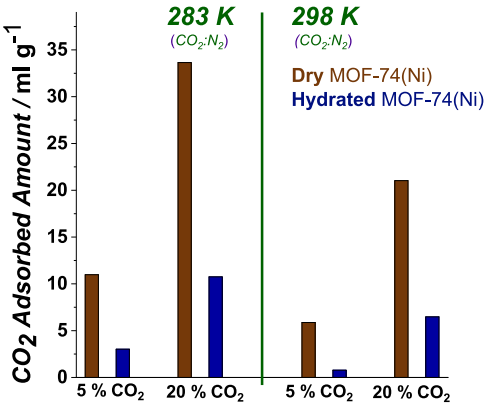

Figure 7. Amount of gas adsorbed on MOF-74(Ni) (dry and hydrated) calculated from breakthrough profiles at 1 bar (absolute pressure) for CO_2:N_2, at different concentrations (CO_2: 5−20%), and different temperatures (283−298 K). Time zero is set with the first detection of helium (tracer).

show the competitive adsorption of water in MOF-74(Ni). This resulted in a drastic decrease in the CO_2 adsorption capacity and thus in its separation efficiency in the presence of water. The same trend is observed at all tested gas compositions and temperatures.

Regarding the related DABCO pillared MOFs [M_2(1,4-bdc)$_2$(DABCO)] (M = Ni, Zn), both materials show good CO_2:N_2 selectivities, but they collapse in a humid environment.[63] Although these MOFs do not contain free coordination sites for water to readily interact with, they are not stable under >60% relative humidity at RT. Degradation seems to be related to water adsorption at defect sites in the MOFs.[64] Considering water one of the most common contaminants, the possibility of performance in its presence is a relevant parameter for implementation in the current separation industry.

CONCLUSIONS

This carborane-based material (***m*CB-MOF-1**) presents not only competitive capacity and remarkable selectivity values for carbon dioxide adsorption in CO_2:N_2 mixtures, but it also stands for its excellent water stability along the separation process. The presence of unsaturated open metal sites explains the higher selectivity for CO_2 sorption than that for N_2. H_2O is excluded from the pores due to the high hydrophobicity of our MOF.

After testing the adsorbent in different concentrations, temperatures, and humid conditions, two statements highlight the potential of this adsorbent: (i) the sieving effect derives in complete gas separation, achieving high CO_2 capture efficiency, but allowing complete regeneration at mild

https://doi.org/10.1021/acsami.2c20373
ACS Appl. Mater. Interfaces 2023, 15, 5309−5316

conditions; and (ii) adsorption properties remain constant under moisture conditions, placing ***m*CB-MOF-1** as an interesting alternative in separation processes involving an extreme humidity atmosphere. Given the mild affinity between gas and adsorbent ***m*CB-MOF-1**, the gas separation with higher CO_2 concentration at a lower temperature is specifically suitable for industrial purification processes over highly contaminated flows.

In addition, MOF-74(Ni) has been used as a reference due to its water stability properties; ***m*CB-MOF-1** surpasses its performance and suppresses the rest of competitors in such challenging moisture operation conditions.

EXPERIMENTAL SECTION

Materials. All chemicals were of reagent-grade quality. They were purchased from commercial sources and used as received. ***m*CB-MOF-1** was synthesized as previously reported.[52] Crystals of ***m*CB-MOF-1** were immersed in acetone and exchanged once a day for three consecutive days, then filtered, and dried in air. The latter were then activated by heating at 120 °C under a dynamic vacuum for 2h.

Characterization and Methods. Gas sorption−desorption measurements were performed using IGA001 and ASAP2020 surface area analyzers. The sample was first degassed at 130 °C for 12 h. Powder X-ray diffraction (PXRD) was recorded at room temperature on a Siemens D-5000 diffractometer with Cu Kα radiation (λ = 1.54056 Å, 45 kV, 35 mA, increment = 0.02°).

The isothermal parameters were well fitted by the double-site Langmuir−Freundlich (DSLF) method from the pure CO_2 adsorption isotherms at 273 K. Fitting parameters of these equations as well as the correlation coefficients (R^2) are listed in Table S1. Predicted selectivity for binary mixtures of CO_2/N_2 was analyzed using IAST.

Ideal Adsorbed Solution Theory (IAST) selectivity. To investigate the separation efficiency of CO_2:N_2 mixtures for ***m*CB-MOF-1**, the IAST method was used to predict the molar loadings at specific partial pressures using pure single-component isotherm fits.

For the adsorption isotherm of CO_2 and N_2 on ***m*CB-MOF-1**' at 273 K, it was fitted with a double-site Langmuir−Freundlich (DSLF) model

$$q = \frac{q_{sat,}\ 1 b_1 p^{c_1}}{1 + b_1 p^{c_1}} + \frac{q_{sat,}\ 2 b_2 p^{c_2}}{1 + b_2 p^{c_2}}$$

Here, $q_{sat,1}$ and $q_{sat,2}$ are saturation uptake (mmol/g) for sites 1 and 2, respectively; b_1 and b_2 are the affinity coefficients of sites 1 and 2, respectively; and c_1 and c_2 are the parameters for the deviations of an ideal homogeneous surface, respectively.

In the Ideal Adsorbed Solution Theory (IAST), two-gas adsorption selectivity could be calculated from single-component isotherm fitting parameters, defined as follows

$$S_{ads} = \frac{q_1/q_2}{p_1/p_2}$$

Isosteric Heat of Adsorption. To evaluate the interactions between ***m*CB-MOF-1** and these gas molecules (CO_2 and N_2), the isosteric heat of adsorption Q_{st} was calculated. In detail, Q_{st} was obtained by fitting adsorption isotherms of CO_2 at 273, 298, and 303 K and N_2 at 77 and 313 K with eq 1. Then, Q_{st} was calculated by eq 2.

$$\ln p = \ln N + \left(\frac{1}{T}\right)\sum_{i=0}^{m} a_i N^i + \sum_{j=0}^{n} b_j N^j \quad (1)$$

$$Q_{st} = -R\sum_{i=0}^{m} a_i N^i \quad (2)$$

where p and N are the pressure (Torr) and the quantity adsorbed (mg/g), respectively; T is the temperature (K); a_i and b_j are empirical parameters, respectively; m and n are the number of coefficients required to give a good fit to the isotherms, respectively; and R is the ideal gas constant ($J{\cdot}K^{-1}{\cdot}mol^{-1}$).

Breakthrough Separation Experiments. Dynamic breakthrough experiments were done on an ABR (*HIDEN Isochema*) instrument. It is an automated breakthrough analyzer based on a fixed-bed adsorption column. In a typical experiment, pressure, temperature, and inlet composition are set and controlled. To determine the adsorption dynamic behavior of gas mixtures, the outlet flow composition is analyzed by an integrated mass spectrometer (HPR-20 *QIC*). The column was filled with 224 mg of ***m*CB-MOF-1**. Before every measurement, the sample was regenerated at atmospheric temperature and pressure in 15 mL min^{-1} Ar flow for 20 min. Operation conditions ranged from 283 to 298 K at 1 bar. The inlet gases mixtures consisted of a 15 mL min^{-1} dilution of carbon dioxide in nitrogen (5−20% CO_2 in N_2). In all situations, gas mixtures resemble expected natural or industrial compositions. Time zero, in the analysis, is set with the first detection of helium due to its use as a tracer (1 mL min^{-1} of He in the feed flow). When using wet-gas mixtures, it was introduced as a moisture desiccator after the column to avoid any damage to the instrument or the mass spectrometer. Any effect derived from the introduction of these elements was corrected with a blank measurement.

ASSOCIATED CONTENT

Supporting Information

The Supporting Information is available free of charge at https://pubs.acs.org/doi/10.1021/acsami.2c20373.

Langmuir−Freundlich fitting parameters, breakthrough curves, experimental dynamic values, and XRD spectra (PDF)

AUTHOR INFORMATION

Corresponding Authors

Guillermo Mínguez Espallargas − *Instituto de Ciencia Molecular (ICMol), Universidad de Valencia, 46980 Paterna, Spain;* orcid.org/0000-0001-7855-1003; Email: guillermo.minguez@uv.es

José Giner Planas − *Institut de Ciència de Materials de Barcelona (ICMAB-CSIC), 08193 Bellaterra, Spain;* orcid.org/0000-0002-1648-2169; Email: jginerplanas@icmab.es

Authors

Lei Gan − *Institut de Ciència de Materials de Barcelona (ICMAB-CSIC), 08193 Bellaterra, Spain;* orcid.org/0000-0002-4230-3662

Eduardo Andres-Garcia − *Instituto de Ciencia Molecular (ICMol), Universidad de Valencia, 46980 Paterna, Spain*

Complete contact information is available at: https://pubs.acs.org/10.1021/acsami.2c20373

Author Contributions

[§]L.G. and E.A.-G. equal contribution.

Notes

The authors declare no competing financial interest.

ACKNOWLEDGMENTS

The work has been supported by the European Union (ERC-2016-CoG 724681-S-CAGE), MINECO PID2019-106832RB-100, and PID2020-117177GB-I00 grants, CEX2019-000919-M, funded by MCIN/AEI/10.13039/501100011033, the Generalitat Valenciana (PROMETEO program), and the Generalitat de Catalunya (2017/SGR/1720). L.G. acknowl-

edges the China Scholarship Council (CSC) for his Ph.D. grant (201808310071). E.A.-G thanks MICINN for a Juan de la Cierva Formación fellowship (FJC2019-039015-I) and for a Margarita Salas Requalification Programme (MS21-035). This study forms part of the Advanced Materials program and was supported by MCIN with funding from European Union NextGenerationEU (PRTR-C17.I1) and by Generalitat Valenciana (project MAF/2022/31).

REFERENCES

(1) Yang, H.; Xu, Z.; Fan, M.; Gupta, R.; Slimane, R. B.; Bland, A. E.; Wright, I. Progress in Carbon Dioxide Separation and Capture: A Review. *J. Environ. Sci.* **2008**, *20*, 14−27.
(2) IEA, *Global Energy Review 2021*, IEA: Paris, 2021.
(3) Singh, D.; Croiset, E.; Douglas, P. L.; Douglas, M. A. Techno-Economic Study of CO2 Capture from an Existing Coal-Fired Power Plant: MEA Scrubbing vs. O2/CO2 Recycle Combustion. *Energy Convers. Manag.* **2003**, *44*, 3073−3091.
(4) Yeh, J. T.; Resnik, K. P.; Rygle, K.; Pennline, H. W. Semi-Batch Absorption and Regeneration Studies for CO2 Capture by Aqueous Ammonia. *Fuel Process. Technol.* **2005**, *86*, 1533−1546.
(5) Yamasaki, A. An Overview of CO₂ Mitigation Options for Global Warming—Emphasizing CO₂ Sequestration Options. *J. Chem. Eng. Jpn.* **2003**, *36*, 361−375.
(6) Xu, X.; Song, C.; Andresen, J. M.; Miller, B. G.; Scaroni, A. W. Novel Polyethylenimine-Modified Mesoporous Molecular Sieve of MCM-41 Type as High-Capacity Adsorbent for CO2 Capture. *Energy Fuels* **2002**, *16*, 1463−1469.
(7) Rodrigues, M. A.; de Souza Ribeiro, J.; de Miranda, J. L.; Ferraz, H. C. Nanostructured Membranes Containing UiO-66 (Zr) and MIL-101 (Cr) for O2/N2 and CO2/N2 Separation. *Sep. Purif. Technol.* **2018**, *192*, 491−500.
(8) Jian, Y.; Yin, H.; Chang, F.; Cheng, L.; Yang, J.; Mu, W.; Li, X.; Lu, J.; Zhang, Y.; Wang, J. Facile Synthesis of Highly Permeable CAU-1 Tubular Membranes for Separation of CO2/N2 Mixtures. *J. Memb. Sci.* **2017**, *522*, 140−150.
(9) Rocha, L. A. M.; Andreassen, K. A.; Grande, C. A. Separation of CO2/CH4 Using Carbon Molecular Sieve (CMS) at Low and High Pressure. *Chem. Eng. Sci.* **2017**, *164*, 148−157.
(10) Hu, Z.; Gami, A.; Wang, Y.; Zhao, D. A Triphasic Modulated Hydrothermal Approach for the Synthesis of Multivariate Metal−Organic Frameworks with Hydrophobic Moieties for Highly Efficient Moisture-Resistant CO2 Capture. *Adv. Sustainable Syst.* **2017**, *1*, No. 1700092.
(11) Grande, C. A.; Roussanaly, S.; Anantharaman, R.; Lindqvist, K.; Singh, P.; Kemper, J. CO2 Capture in Natural Gas Production by Adsorption Processes. *Energy Procedia* **2017**, *114*, 2259−2264.
(12) Akten, E. D.; Siriwardane, R.; Sholl, D. S. Monte Carlo Simulation of Single- and Binary-Component Adsorption of CO2, N2, and H2 in Zeolite Na-4A. *Energy Fuels* **2003**, *17*, 977−983.
(13) Belmabkhout, Y.; Serna-Guerrero, R.; Sayari, A. Adsorption of CO2 from Dry Gases on MCM-41 Silica at Ambient Temperature and High Pressure. 1: Pure CO2 Adsorption. *Chem. Eng. Sci.* **2009**, *64*, 3721−3728.
(14) Choi, B.-U.; Choi, D.-K.; Lee, Y.-W.; Lee, B.-K.; Kim, S.-H. Adsorption Equilibria of Methane, Ethane, Ethylene, Nitrogen, and Hydrogen onto Activated Carbon. *J. Chem. Eng. Data* **2003**, *48*, 603−607.
(15) Nugent, P.; Belmabkhout, Y.; Burd, S. D.; Cairns, A. J.; Luebke, R.; Forrest, K.; Pham, T.; Ma, S.; Space, B.; Wojtas, L.; Eddaoudi, M.; Zaworotko, M. J. Porous Materials with Optimal Adsorption Thermodynamics and Kinetics for CO2 Separation. *Nature* **2013**, *495*, 80−84.
(16) Lv, D.; Wang, H.; Chen, Y.; Xu, F.; Shi, R.; Liu, Z.; Wang, X.; Teat, S. J.; Xia, Q.; Li, Z.; Li, J. Iron-Based Metal−Organic Framework with Hydrophobic Quadrilateral Channels for Highly Selective Separation of Hexane Isomers. *ACS Appl. Mater. Interfaces* **2018**, *10*, 6031−6038.
(17) Chen, Y.; Wu, H.; Liu, Z.; Sun, X.; Xia, Q.; Li, Z. Liquid-Assisted Mechanochemical Synthesis of Copper Based MOF-505 for the Separation of CO2 over CH4 or N2. *Ind. Eng. Chem. Res.* **2018**, *57*, 703−709.
(18) Liang, L.; Chen, Q.; Jiang, F.; Yuan, D.; Qian, J.; Lv, G.; Xue, H.; Liu, L.; Jiang, H.-L.; Hong, M. In Situ Large-Scale Construction of Sulfur-Functionalized Metal−Organic Framework and Its Efficient Removal of Hg(Ii) from Water. *J. Mater. Chem. A* **2016**, *4*, 15370−15374.
(19) Kizzie, A. C.; Wong-Foy, A. G.; Matzger, A. J. Effect of Humidity on the Performance of Microporous Coordination Polymers as Adsorbents for CO2 Capture. *Langmuir* **2011**, *27*, 6368−6373.
(20) Álvarez, J. R.; Sánchez-González, E.; Pérez, E.; Schneider-Revueltas, E.; Martínez, A.; Tejeda-Cruz, A.; Islas-Jácome, A.; González-Zamora, E.; Ibarra, I. A. Structure Stability of HKUST-1 towards Water and Ethanol and Their Effect on Its CO2 Capture Properties. *Dalton Trans.* **2017**, *46*, 9192−9200.
(21) Álvarez, J. R.; Sánchez-González, E.; Pérez, E.; Schneider-Revueltas, E.; Martínez, A.; Tejeda-Cruz, A.; Islas-Jácome, A.; González-Zamora, E.; Ibarra, I. A. Structure Stability of HKUST-1 towards Water and Ethanol and Their Effect on Its CO2 Capture Properties. *Dalton Trans.* **2017**, *46*, 9192−9200.
(22) Ming, Y.; Purewal, J.; Yang, J.; Xu, C.; Soltis, R.; Warner, J.; Veenstra, M.; Gaab, M.; Müller, U.; Siegel, D. J. Kinetic Stability of MOF-5 in Humid Environments: Impact of Powder Densification, Humidity Level, and Exposure Time. *Langmuir* **2015**, *31*, 4988−4995.
(23) Chen, K.-J.; Madden, D. G.; Pham, T.; Forrest, K. A.; Kumar, A.; Yang, Q.-Y.; Xue, W.; Space, B.; Perry, J. J., IV; Zhang, J.-P.; Chen, X.-M.; Zaworotko, M. J. Tuning Pore Size in Square-Lattice Coordination Networks for Size-Selective Sieving of CO2. *Angew. Chem., Int. Ed.* **2016**, *55*, 10268−10272.
(24) Bhatt, P. M.; Belmabkhout, Y.; Cadiau, A.; Adil, K.; Shekhah, O.; Shkurenko, A.; Barbour, L. J.; Eddaoudi, M. A Fine-Tuned Fluorinated MOF Addresses the Needs for Trace CO2 Removal and Air Capture Using Physisorption. *J. Am. Chem. Soc.* **2016**, *138*, 9301−9307.
(25) Shekhah, O.; Belmabkhout, Y.; Chen, Z.; Guillerm, V.; Cairns, A.; Adil, K.; Eddaoudi, M. Made-to-Order Metal-Organic Frameworks for Trace Carbon Dioxide Removal and Air Capture. *Nat. Commun.* **2014**, *5*, No. 4228.
(26) Shi, Z.; Tao, Y.; Wu, J.; Zhang, C.; He, H.; Long, L.; Lee, Y.; Li, T.; Zhang, Y.-B. Robust Metal−Triazolate Frameworks for CO2 Capture from Flue Gas. *J. Am. Chem. Soc.* **2020**, *142*, 2750−2754.
(27) Li, L.-J.; Liao, P.-Q.; He, C.-T.; Wei, Y.-S.; Zhou, H.-L.; Lin, J.-M.; Li, X.-Y.; Zhang, J.-P. Grafting Alkylamine in UiO-66 by Charge-Assisted Coordination Bonds for Carbon Dioxide Capture from High-Humidity Flue Gas. *J. Mater. Chem. A* **2015**, *3*, 21849−21855.
(28) Xian, S.; Wu, Y.; Wu, J.; Wang, X.; Xiao, J. Enhanced Dynamic CO2 Adsorption Capacity and CO2/CH4 Selectivity on Polyethylenimine-Impregnated UiO-66. *Ind. Eng. Chem. Res.* **2015**, *54*, 11151−11158.
(29) Chen, T.-H.; Popov, I.; Zenasni, O.; Daugulis, O.; Miljanić, O. Š. Superhydrophobic Perfluorinated Metal−Organic Frameworks. *Chem. Commun.* **2013**, *49*, 6846−6848.
(30) Padial, N. M.; Quartapelle Procopio, E.; Montoro, C.; López, E.; Oltra, J. E.; Colombo, V.; Maspero, A.; Masciocchi, N.; Galli, S.; Senkovska, I.; Kaskel, S.; Barea, E.; Navarro, J. A. R. Highly Hydrophobic Isoreticular Porous Metal−Organic Frameworks for the Capture of Harmful Volatile Organic Compounds. *Angew. Chem., Int. Ed.* **2013**, *52*, 8290−8294.
(31) Nguyen, J. G.; Cohen, S. M. Moisture-Resistant and Superhydrophobic Metal−Organic Frameworks Obtained via Post-synthetic Modification. *J. Am. Chem. Soc.* **2010**, *132*, 4560−4561.
(32) Scholz, M.; Hey-Hawkins, E. Carbaboranes as Pharmacophores: Properties, Synthesis, and Application Strategies. *Chem. Rev.* **2011**, *111*, 7035−7062.
(33) Grimes, R. N. Carboranes in the Chemist's Toolbox. *Dalt. Trans.* **2015**, *44*, 5939−5956.

https://doi.org/10.1021/acsami.2c20373
ACS Appl. Mater. Interfaces 2023, 15, 5309−5316

(34) Teixidor, F.; Viñas, C. In *Science of Synthesis*, D E, K.; D S, M., Eds.; Thieme: Stuttgart, 2005; Vol. *6*, pp 1275−1325.
(35) Poater, J.; Solà, M.; Viñas, C.; Teixidor, F. π Aromaticity and Three-Dimensional Aromaticity: Two Sides of the Same Coin. *Angew. Chem. Int. Ed.* **2014**, *53*, 12191−12195.
(36) Poater, J.; Viñas, C.; Bennour, I.; Escayola, S.; Solà, M.; Teixidor, F. Too Persistent to Give Up: Aromaticity in Boron Clusters Survives Radical Structural Changes. *J. Am. Chem. Soc.* **2020**, *142*, 9396−9407.
(37) Poater, J.; Viñas, C.; Solà, M.; Teixidor, F. 3D and 2D Aromatic Units Behave like Oil and Water in the Case of Benzocarborane Derivatives. *Nat. Commun.* **2022**, *13*, No. 3844.
(38) Farha, O. K.; Spokoyny, A. M.; Mulfort, K. L.; Hawthorne, M. F.; Mirkin, C. A.; Hupp, J. T. Synthesis and Hydrogen Sorption Properties of Carborane Based Metal−Organic Framework Materials. *J. Am. Chem. Soc.* **2007**, *129*, 12680−12681.
(39) Bae, Y.-S.; Farha, O. K.; Spokoyny, A. M.; Mirkin, C. A.; Hupp, J. T.; Snurr, R. Q. Carborane-Based Metal−Organic Frameworks as Highly Selective Sorbents for CO2 over Methane. *Chem. Commun.* **2008**, *35*, 4135.
(40) Farha, O. K.; Spokoyny, A. M.; Mulfort, K. L.; Galli, S.; Hupp, J. T.; Mirkin, C. A. Gas-Sorption Properties of Cobalt(II)−Carborane-Based Coordination Polymers as a Function of Morphology. *Small* **2009**, *5*, 1727−1731.
(41) Spokoyny, A. M.; Farha, O. K.; Mulfort, K. L.; Hupp, J. T.; Mirkin, C. A. Porosity Tuning of Carborane-Based Metal−Organic Frameworks (MOFs) via Coordination Chemistry and Ligand Design. *Inorganica Chim. Acta* **2010**, *364*, 266−271.
(42) Bae, Y.-S.; Spokoyny, A. M.; Farha, O. K.; Snurr, R. Q.; Hupp, J. T.; Mirkin, C. A. Separation of Gas Mixtures Using Co(Ii) Carborane-Based Porous Coordination Polymers. *Chem. Commun.* **2010**, *46*, 3478−3480.
(43) Kennedy, R. D.; Krungleviciute, V.; Clingerman, D. J.; Mondloch, J. E.; Peng, Y.; Wilmer, C. E.; Sarjeant, A. A.; Snurr, R. Q.; Hupp, J. T.; Yildirim, T.; Farha, O. K.; Mirkin, C. A. Carborane-Based Metal−Organic Framework with High Methane and Hydrogen Storage Capacities. *Chem. Mater.* **2013**, *25*, 3539−3543.
(44) Spokoyny, A. M. New Ligand Platforms Featuring Boron-Rich Clusters as Organomimetic Substituents. *Pure Appl. Chem.* **2013**, *85*, 903−919.
(45) Clingerman, D. J.; Morris, W.; Mondloch, J. E.; Kennedy, R. D.; Sarjeant, A. A.; Stern, C.; Hupp, J. T.; Farha, O. K.; Mirkin, C. A. Stabilization of a Highly Porous Metal−Organic Framework Utilizing a Carborane-Based Linker. *Chem. Commun.* **2015**, *51*, 6521−6523.
(46) Para-Carborane Is about Five Times More Expensive than Ortho- and Meta-Carborane; Source Katchem Ltd., 2022.
(47) Rodríguez-Hermida, S.; Tsang, M. Y.; Vignatti, C.; Stylianou, K. C.; Guillerm, V.; Pérez-Carvajal, J.; Teixidor, F.; Viñas, C.; Choquesillo-Lazarte, D.; Verdugo-Escamilla, C.; Peral, I.; Juanhuix, J.; Verdaguer, A.; Imaz, I.; Maspoch, D.; Giner Planas, J. Switchable Surface Hydrophobicity-Hydrophilicity of a Metal-Organic Framework. *Angew. Chem., Int. Ed.* **2016**, *55*, 16049−16053.
(48) Soldevila-Sanmartín, J.; Ruiz, E.; Choquesillo-Lazarte, D.; Light, M. E.; Viñas, C.; Teixidor, F.; Núñez, R.; Pons, J.; Planas, G.; Tuning, J. the Architectures and Luminescence Properties of Cu(<scp>i</Scp>) Compounds of Phenyl and Carboranyl Pyrazoles: The Impact of 2D versus 3D Aromatic Moieties in the Ligand Backbone. *J. Mater. Chem. C* **2021**, *9*, 7643−7657.
(49) Tsang, M. Y.; Rodríguez-Hermida, S.; Stylianou, K. C.; Tan, F.; Negi, D.; Teixidor, F.; Viñas, C.; Choquesillo-Lazarte, D.; Verdugo-Escamilla, C.; Guerrero, M.; Sort, J.; Juanhuix, J.; Maspoch, D.; Giner Planas, J. Carborane Bis-Pyridylalcohols as Linkers for Coordination Polymers: Synthesis, Crystal Structures, and Guest-Framework Dependent Mechanical Properties. *Cryst. Growth Des.* **2017**, *17*, 846−857.
(50) Tan, F.; López-Periago, A.; Light, M. E.; Cirera, J.; Ruiz, E.; Borrás, A.; Teixidor, F.; Viñas, C.; Domingo, C.; Planas, J. G. An Unprecedented Stimuli-Controlled Single-Crystal Reversible Phase Transition of a Metal−Organic Framework and Its Application to a Novel Method of Guest Encapsulation. *Adv. Mater.* **2018**, *30*, No. 1800726.
(51) Gan, L.; Fonquernie, P. G.; Light, M. E.; Norjmaa, G.; Ujaque, G.; Choquesillo-Lazarte, D.; Fraile, J.; Teixidor, F.; Viñas, C.; Planas, J. G. A Reversible Phase Transition of 2D Coordination Layers by B−H•••Cu(II) Interactions in a Coordination Polymer. *Molecules* **2019**, *24*, 3204.
(52) Gan, L.; Chidambaram, A.; Fonquernie, P. G.; Light, M. E.; Choquesillo-Lazarte, D.; Huang, H.; Solano, E.; Fraile, J.; Viñas, C.; Teixidor, F.; Navarro, J. A. R.; Stylianou, K. C.; Planas, J. G. A Highly Water-Stable Meta -Carborane-Based Copper Metal−Organic Framework for Efficient High-Temperature Butanol Separation. *J. Am. Chem. Soc.* **2020**, *142*, 8299−8311.
(53) Li, Z.; Fraile, J.; Viñas, C.; Teixidor, F.; Planas, J. G. Post-Synthetic Modification of a Highly Flexible 3D Soft Porous Metal−Organic Framework by Incorporating Conducting Polypyrrole: Enhanced MOF Stability and Capacitance as an Electrode Material. *Chem. Commun.* **2021**, *57*, 2523−2526.
(54) Li, Z.; Choquesillo-Lazarte, D.; Fraile, J.; Viñas, C.; Teixidor, F.; Planas, J. G. Rational Design of Carborane-Based Cu 2 -Paddle Wheel Coordination Polymers for Increased Hydrolytic Stability. *Dalt. Trans.* **2022**, *51*, 1137−1143.
(55) Li, Z.; Núñez, R.; Light, M. E.; Ruiz, E.; Teixidor, F.; Viñas, C.; Ruiz-Molina, D.; Roscini, C.; Planas, J. G. Water-Stable Carborane-Based Eu3+/Tb3+ Metal−Organic Frameworks for Tunable Time-Dependent Emission Color and Their Application in Anticounterfeiting Bar-Coding. *Chem. Mater.* **2022**, *34*, 4795−4808.
(56) Dybtsev, D. N.; Chun, H.; Kim, K. Rigid and Flexible: A Highly Porous Metal−Organic Framework with Unusual Guest-Dependent Dynamic Behavior. *Angew. Chem., Int. Ed.* **2004**, *43*, 5033−5036.
(57) Maniam, P.; Stock, N. Investigation of Porous Ni-Based Metal−Organic Frameworks Containing Paddle-Wheel Type Inorganic Building Units via High-Throughput Methods. *Inorg. Chem.* **2011**, *50*, 5085−5097.
(58) Bhunia, M. K.; Hughes, J. T.; Fettinger, J. C.; Navrotsky, A. Thermochemistry of Paddle Wheel MOFs: Cu-HKUST-1 and Zn-HKUST-1. *Langmuir* **2013**, *29*, 8140−8145.
(59) Mason, J. A.; Sumida, K.; Herm, Z. R.; Krishna, R.; Long, J. R. Evaluating Metal−Organic Frameworks for Post-Combustion Carbon Dioxide Capture via Temperature Swing Adsorption. *Energy Environ. Sci.* **2011**, *4*, 3030−3040.
(60) Zeng, H.; Qu, X.; Xu, D.; Luo, Y.Porous Adsorption Materials for Carbon Dioxide Capture in Industrial Flue Gas*Front. Chem.*2022, *10*, DOI: 10.3389/fchem.2022.939701.
(61) Voskanyan, A. A.; Goncharov, V. G.; Novendra, N.; Guo, X.; Navrotsky, A. Thermodynamics Drives the Stability of the MOF-74 Family in Water. *ACS Omega* **2020**, *5*, 13158−13163.
(62) Liu, J.; Benin, A. I.; Furtado, A. M. B.; Jakubczak, P.; Willis, R. R.; LeVan, M. D. Stability Effects on CO2 Adsorption for the DOBDC Series of Metal−Organic Frameworks. *Langmuir* **2011**, *27*, 11451−11456.
(63) Liang, Z.; Marshall, M.; Chaffee, A. L. CO2 Adsorption, Selectivity and Water Tolerance of Pillared-Layer Metal Organic Frameworks. *Microporous Mesoporous Mater.* **2010**, *132*, 305−310.
(64) Chen, C.; Yu, Z.; Sholl, D. S.; Walton, K. S. Effect of Loading on the Water Stability of the Metal−Organic Framework DMOF-1 [Zn(Bdc)(Dabco)0.5]. *J. Phys. Chem. Lett.* **2022**, *13*, 4891−4896.